Experimental Demonstrations of High-Capacity THz-Wireless Transmission Systems for Beyond 5G

Carlos Castro, Robert Elschner, Thomas Merkle, Colja Schubert, and Ronald Freund

Abstract

Using the concept of a "THz-wireless fiber extender," we can combine the flexibility of wireless networks with the high capacity of fiber optic communication. The availability of a large, contiguous bandwidth in the frequency band around 300 GHz creates the opportunity to seamlessly interconnect coherent THz-wireless and fiber optic transceiver frontends using a transparent, analog baseband interface. In this article, we discuss this concept in more detail and report on the recent demonstration of a real-time, short-range THz-wireless fiber extender with 100 Gb/s net capacity. This combined fiber optic/THz-wireless transmission system is operated by a high-speed fiber optic real-time modem, which is capable of compensating the channel impairments of both the optical and THz-wireless links. In addition, we discuss the potential of THz-wireless links to achieve long-range transmission distances by reporting on the operation of a 500-m-long line-of-sight THz-wireless outdoor link in Berlin, Germany. We analyze the effect of weather conditions on the transmission performance and determine the maximum physical layer net data rate of the system by means of various modulation formats and symbol rates. Finally, we summarize all of our recent high-capacity experiments using THz-wireless transmission, including a field trial with a 1-km-long link, and compare our results to theoretical limits and achieved data rates in the laboratory.

Introduction

In the last few decades, we have seen how modern society has transformed toward an interconnected world, in which remote data access is a commodity, and machine-centric applications such as Industry 4.0 and autonomous vehicles require a reliable, flexible, low-latency network that can handle large amounts of data at increasing transfer rates. The evolution of mobile networks has caused a proliferation of connected users and mobile devices, which will continue to increase rapidly in the coming years due to the advent of the Internet of Things [1]. To support the future requirements of new use cases such as enhanced mobile broadband, ultra-reliable low-latency communication, and massive machine type communications, many service providers have started to deploy network elements of the fifth generation (5G), enabled by communication concepts such as massive multiple-input multiple-output (mMIMO) systems, smaller cells, and millimeter-wave transmission [2].

Despite promising enormous data rates, 5G is still bound by regulations to a relatively small portion of the electromagnetic spectrum. For this reason, researchers are already investigating new core technologies that can possibly provide more bandwidth to improve on 5G's capabilities. A possible candidate may be THz-wireless communications, in which data is modulated onto carrier frequencies in the spectral region that starts at 0.1 THz and extends into the THz frequency range. One of the most appealing characteristics of THz communications is the available wide and contiguous bandwidth, which promises net data rates above 100 Gb/s for a single wireless physical layer link [3]. This creates the unique opportunity to seamlessly combine THz wireless technologies with the existing fiber optic infrastructure to achieve enhanced network flexibility. With such THz-wireless fiber extenders [4], it is possible to interconnect areas where network infrastructure was previously missing due to budget or geographical difficulties.

While at first glance it may appear that a competing technology such as free-space optics (FSO) is more suitable for integration with optical links based on available bandwidth and transparency, THz technologies offer some distinct advantages over FSO: a time-invariant, stable, and flat channel, not affected by atmospheric turbulence, and the possibility to use single-carrier digital signal processing (DSP) strategies, and also compact, cost-effective, electronics-based front-ends without the need for adaptive optics.

For such reasons, several demonstrations on high-speed single-channel transmission in the THz band have been carried out, typically relying on photonic up-conversion techniques to generate the modulated THz signal [5–8].

In contrast, our approach is based on electronic THz up- and down-conversion using monolithic microwave integrated circuits. This has allowed us to demonstrate a THz-wireless fiber extender

Using the concept of a "THz-wireless fiber extender," we can combine the flexibility of wireless networks with the high capacity of fiber-optical communication. The availability of a large, contiguous bandwidth in the frequency band around 300 GHz creates the opportunity to seamlessly interconnect coherent THz-wireless and fiber optic transceiver frontends using a transparent, analog baseband interface.

Carlos Castro, Robert Elschner, Colja Schubert, and Ronald Freund are with the Fraunhofer Heinrich Hertz Institute; Thomas Merkle is with the Fraunhofer Institute for Applied Solid-State Physics.

Digital Object Identifier: 10.1109/MCOM.001.2000306

One of the most likely immediate use cases for the THz-wireless communications technology is to support the extension of an existing network infrastructure where it is not economically or technically feasible to install new optical fibers.

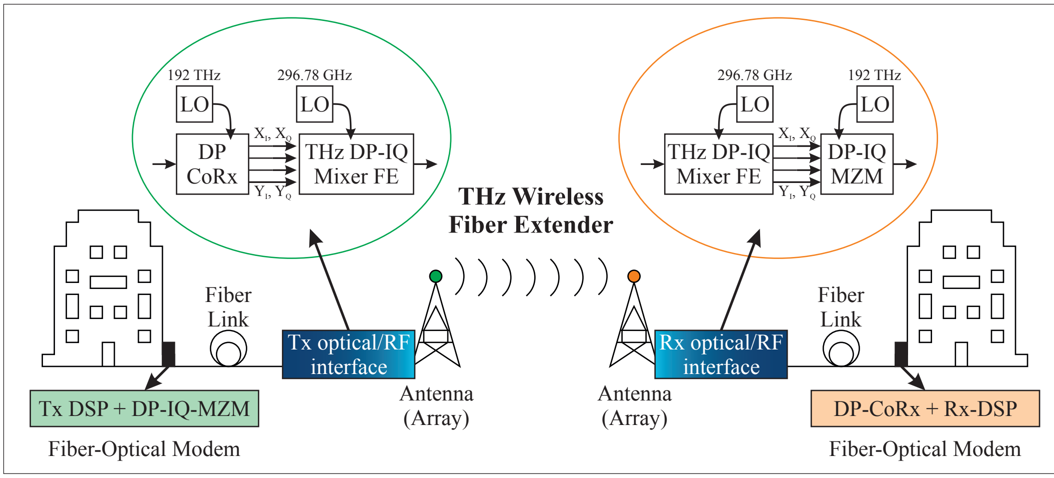

Figure 1. Concept of a unidirectional THz-wireless fiber extender. The optical/RF interfaces comprise analog coherent baseband front-ends that allow direct conversion from the fiber optic domain to the electrical baseband (XI, XQ, YI, YQ) and further to the THz-wireless domain without local DSP, and vice versa. At the receiver side, a single DSP chain jointly corrects the transmission impairments that originate from both the fiber optic and THz-wireless domains.

concept compatible with commercial off-the-shelf fiber optic components, with the idea of using those synergies to reduce cost, shorten development cycles, and simplify market entry in this first technology phase. To this aim, we report on the implementation of a real-time, short-reach fiber optic/THz-wireless system demonstrator in a lab environment as well as on an outdoor, long-range THz-wireless link bridging a distance of 500 m. Both systems achieve a net data rate of 100 Gb/s. Furthermore, we also discuss challenges and required developments toward an integrated THz-wireless fiber extender solution that could be used to realize communication systems beyond 5G.

THz-Wireless Fiber Extender Systems

One of the most likely immediate use cases for the THz-wireless communications technology is to support the extension of an existing network infrastructure where it is not economically or technically feasible to install new optical fibers.

In this regard, developing a concept that combines both transmission strategies (fiber-based and wireless-based) and exploiting the available large, contiguous bandwidth in the THz band, single-carrier THz-wireless technologies appear to be a logically consistent solution. This system architecture has been aptly named THz-wireless bridge or THz-wireless fiber extender [7]. Figure 1 depicts a scenario where the THz-wireless link connects two open-ended fiber optic connections. The cornerstone of this setup is the transparent, analog opto-electrical baseband interface, denoted as "optical/RF interface," which converts the data signals in an analog fashion from the optical domain to the electrical baseband domain and further into the THz band, and vice versa. As the modulated signals travel "transparently" through the combined fiber optic/THz-wireless link, it is possible to use a single fiber optic modem with a typical single-carrier DSP scheme to jointly compensate for all channel impairments from both the optical and THz domains. This requires service providers to perform only minor modifications to their devices and networks. Still, some challenges remain. First, the wireless link will inevitably introduce link loss dynamics due to changing weather conditions, which need to be accounted for by the inclusion of adaptive coding and modulation (ACM) schemes in the fiber optic modem. Second, the polarization-division multiplexing (PDM) scheme, as typically used in digital-coherent fiber optic transmission, also needs to be adapted for the THz-wireless part of the link. Below, we discuss these two challenges together with the demonstration results.

Real-Time 100 Gb/s Transmission over a Combined Fiber Optic/THz-Wireless Link

One of the main research questions regarding THz-wireless fiber extenders is whether the single-carrier DSP of a fiber optic modem can also compensate for the combined effects of both the fiber optic link and THz-wireless link if device imperfections like amplifier/mixer nonlinearities, phase noise, or I/Q imbalances are present, in particular at the optical/RF interface [9]. To answer this question, we implemented a combined fiber optic/THz-wireless link as shown in Fig. 1, which is composed of THz transceiver front-ends (THz DP-IQ Mixer FEs) that operate at an RF carrier frequency of around 300 GHz, analog-coherent optical front-ends (DP-IQ MZM and DP CoRx) operating in optical C-Band around 192 THz, and a real-time high-speed digital-coherent fiber optic modem (Tx-DSP and Rx-DSP), which uses a 34 GBd PDM 4-QAM (quadrature amplitude modulation) scheme [10]. The THz-wireless link is embedded between the two fiber optic links, whose individual lengths can be varied from a couple of meters up to 51.2 km. For both optical fiber sections, the data signal is modulated onto an optical carrier at a frequency of 192 THz and subsequently launched into the fiber at an optical power of 1 dBm.

For short-range indoor lab transmission experiments over a distance of 50 cm, we connected small 23 dBi horn antennas with a diameter of 6.9 mm to the THz-wireless front-ends. At the receiver, the real-time modem, which implements a typical single-carrier DSP similar to [11], is used to mitigate the effects of transmission impairments. The measurement results for the transmission of 34 GBd PDM 4-QAM signals (corresponding to a 136 Gb/s gross bit rate) are depicted in Fig. 2 for different link combinations as a function of the added length of both fiber sections. In our experiments, we covered three possible types of link combinations, depending on where the THz-wireless link is located in relation to the fiber optic links. The total fiber distance was limited to 103 km, because we wanted to focus on a coherent access/metro scenario without in-line optical amplification. The results show that the measured bit error rate (BER) was nearly independent of the actual link combination type and the optical fiber distance. This is because the overall signal-to-noise ratio (SNR) at the receiver, which is directly related to the BER performance, depends on the sum of all noise contributions from the different optical and electrical noise sources. As indicated by simulations of our optic/THz-wireless link, the contribution of the optical noise to the overall SNR was negligible in comparison to the noise contribution from the THz-wireless link in our experimental setup.

The DSP of the real-time modem includes a soft-decision forward error correction (SD-FEC) with a BER threshold of $3.4 \cdot 10^{-2}$ using a FEC overhead of 25 percent. For all measured points, the BER of the real-time system with 100 Gb/s net data rate after overhead removal remained well below this limit, being stable for multiple hours. Thus, the typical fiber optic single-carrier DSP was indeed capable of jointly correcting the combined channel impairments originating from the fiber optic/THz-wireless link: the random polarization rotations occurring at any point of the fiber links, phase noise from both the optical and the THz local oscillators (LOs), and the accumulated chromatic dispersion from the fiber links.

To further verify the linearity and transparency of the optical/RF interface, we also evaluated the accumulated chromatic dispersion that the real-time modem was estimating before correcting it. This metric is plotted in Fig. 2 as a function of the total fiber length, and averaged over the different link combinations. For comparison, the expected values for a standard single-mode fiber with a dispersion parameter of 17 ps/(nm · km) are added to the graph. The agreement between the two curves proves that the single-carrier DSP correctly determines the channel parameters despite introducing a THz-wireless link in the system regardless of the actual link combination type.

In order to further optimize the system performance, it might be worth investigating in a next step to what degree small adjustments of the DSP parameters and the introduction of additional DSP stages improve the operation in terms of bits per second and BER performance. To this extent, we have briefly investigated in offline experiments the introduction of a second, symbol-spaced equalization stage after the carrier phase recovery to particularly compensate for transmitter skew and I/Q imbalances. This modification decreases the measured BER by a factor of 10 compared to that of the real-time system, indicating that there is still potential for improvements [12]. Another challenge will be the introduction of ACM into the fiber optic DSP in order to cope with weather-dependent link loss variations. For single-carrier DSPs, ACM can be achieved by adaptively changing the modulation cardinality, the symbol rate, the FEC overhead, or by probabilistic shaping.

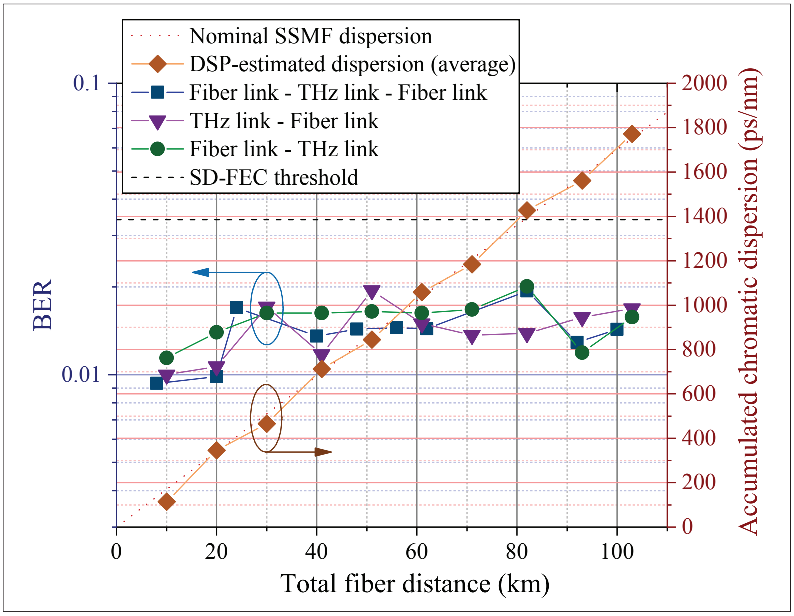

Figure 2. Transmission performance of the THz-wireless fiber extender for different link combinations as a function of the total fiber length. The link combination refers to the position of the THz-wireless link and the fiber link(s) within the transmission line. For example, 'Fiber – THz link– Fiber' means that the THz-wireless link is embedded between two fiber links. Also depicted: the average DSP-estimated chromatic dispersion of the optical link in comparison to the expected result that corresponds to standard single-mode fibers (SSMFs) with a dispersion parameter of 17 ps/(nm · km).

High-Capacity Long-Range THz-Wireless Data Transmission

The large majority of published experiments in the THz-band have focused on short-range indoor experiments, where the technology can be tested without being impacted by changing weather conditions. To realize a real-world implementation of this technology, however, it is necessary to demonstrate that stable THz wireless communication is possible over several hundred meters. Using the same offline DSP scheme applied to the indoor experiments, we constructed a long-range THz-wireless demonstrator in Berlin, Germany [13]. The line-of-sight path spans a distance of 500 m between the main building of the Technical University of Berlin (transmitter) and the Fraunhofer Heinrich Hertz Institute (receiver). The manual alignment was carried out using tripod heads, which can adjust the elevation and azimuth angle with an angular resolution below 1°. To compensate for the high free-space path loss in the 300 GHz band, we employed 55 dBi Cassegrain reflector antennas with an aperture diameter of 225 mm. Furthermore, a weather station at the transmitter site collects data on the atmospheric conditions in order to estimate their impact on the transmission during our experiments.

We designed outdoor units that integrate the THz front-ends, high-gain antennas, and the generation of the 300 GHz local oscillator in a portable housing that simplifies installation and alignment (Fig. 3). The outdoor units also need to protect the electronics from external damage due to dust, rain, heat, and mechanical stress.

The continuously measured BER (over 10 hours of operation) for a single-polarization 32 GBd 4-QAM signal transmission (corresponding to a 64 Gb/s gross bit rate and 51.2 Gb/s net bit rate after removal of the FEC overhead), at a carrier frequency of 296.78 GHz, is shown in Fig. 4. The experiment was carried out on an overcast day in early March 2020. The estimated absolute SNR at the receiver was about 22 dB. Also depicted in the graph is a comparison between the measured variation of the received power (normalized to 0 dB, which corresponds directly to the SNR variation) and the estimation of this variation according to the International Telecommunication Union (ITU) R676-12 Recommendations for modeling the attenuation by atmospheric gases [14]. The model calculation is based on weather data such as atmospheric pressure, temperature, relative humidity, and precipitation rate, which have been recorded by the weather station on a minute-by-minute basis. The plot reveals that, given precise weather data, the ITU model can accurately predict the attenuation along the THz-wireless propagation path; we were even able to reproduce the effects of rapidly changing weather conditions in great detail. A second noteworthy aspect in this graph is the overall stability of the link in terms of received power. The observed variation remains below 1 dB for almost the whole duration of the experiment. The larger fluctuations in the received power were caused by some rain shower events, which also can be noticed in the measured BER. These variations, however, did not exceed the link loss margin, so ACM was not needed in our case. The maximum precipitation rate that we experienced corresponded to ~0.4 mm/h, which is categorized as "light rain." Stronger rain events would have resulted in larger loss variations.

Figure 3. Photograph of the outdoor units at the receiver. The Berlin test site refers to a 500-m-long THz-wireless link between the campus of the Technical University of Berlin and the Fraunhofer Institute for Telecommunications, Heinrich Hertz Institute (HHI). This particular placement of two outdoor units corresponds to a PDM configuration.

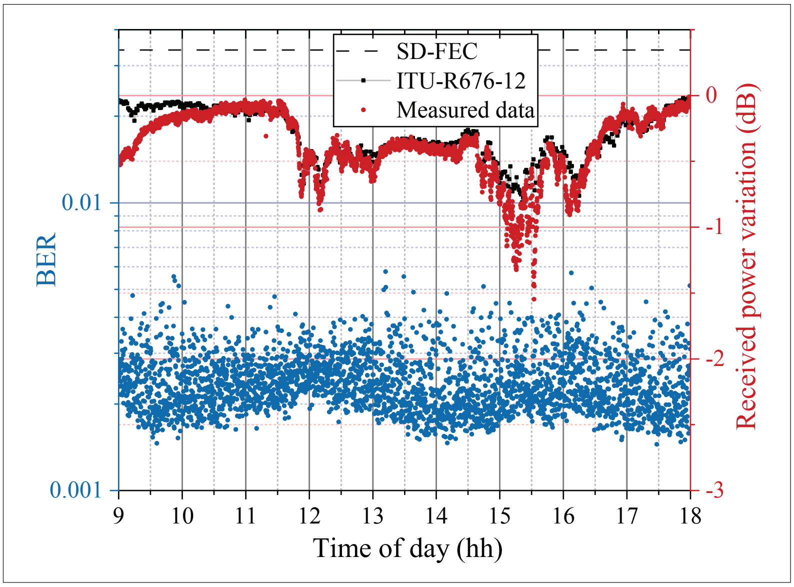

Figure 4. Transmission performance of a 500-m-long THz-wireless link in the 300 GHz band using single-polarization 32 GBd 4-QAM for 10 hours of continuous operation. Also depicted: received power variation arising from weather-dependent atmospheric loss (measured vs. calculated).

Subsequent experiments with the outdoor setup focused on comparing the maximum net data rate that could be achieved for different m-QAM formats. With the limiting condition that the BER stays below the SD-FEC threshold to enable error-free decoding, we were able to transmit 4-QAM at a maximum net data rate of 67.2 Gb/s (42 GBd), 16-QAM at 76.8 Gb/s (24 GBd), and 64-QAM at 38.4 Gb/s (8 GBd); all net data rates are given after removal of the FEC overhead.

In the last experiment, a second Tx/Rx set of THz outdoor units was installed (as shown in Fig. 3), which allows the investigation of THz-wireless data transmission exploiting polarization-division multiplexing. The additional pair of antennas was aligned to support a vertical polarization, whereas the first set was aligned to support a horizontal polarization. In this configuration, we measured the isolation between the vertical and horizontal polarized modes to be greater than 35 dB. With this new configuration, a maximum net data rate of 102.4 Gb/s for a 32-GBd PDM 4-QAM signal was achieved, while keeping the measured BER below the SD-FEC threshold of $3.4 \cdot 10^{-2}$.

Summary of THz-Wireless Transmission Experiments

A summary of our high-capacity transmission experiments is presented in Fig. 5, in which the depicted measurement points refer to a single-polarization configuration of the THz-wireless link unless stated otherwise. In this graph, the data are organized to easily convey the test conditions for the various experiments. In addition, we have introduced reference curves (dotted and dashed lines) in order to represent analytically calculated limits of the THz-wireless system assuming an additive white Gaussian noise (AWGN) channel only characterized by the transmit power, the channel loss, and the receiver noise figure, but otherwise ideal components. The shown reference curves correspond to a BER at the experimentally used SD-FEC threshold of $3.4 \cdot 10^{-2}$.

In the case of short-range transmission (23 dBi gain horn antennas), Fig. 5 shows that for 32 GBd 4-QAM (51.2 Gb/s net data rate), there is still room for improvement, since the maximum distance that we calculated from the AWGN channel is four times larger than what was experimentally observed. This originates from a measured BER value that was noticeably below the SD-FEC threshold. On the other hand, the gap between the experimental 16-QAM transmission to its reference curve is smaller, less than a factor of two, because the transmission performance of that experiment was closer to the SD-FEC limit. The remaining differences are attributed mainly to implementation penalties due to component bandwidth limitations, and amplifier and mixer nonlinearities at the THz front-ends, which affect high-order modulation formats more severely.

For the long-range experiments, we have tried to collect data as close as possible to the SD-FEC limit to isolate the implementation penalties due to atmospheric losses and the imperfections of the THz front-ends. Besides the dataset corresponding to the 500-m-long link in Berlin, we also have plotted the results of transmission experiments using a 1-km-long THz-wireless link, which we set up in Freiburg, Germany, in early September 2019. This earlier experiment with 32 GBd 4-QAM signals (44.8 Gb/s net data rate) serves to demonstrate the potential of high-capacity transmission in the THz band over larger distances in the kilometer range. For the 500-m-long link in Berlin, the data points corresponding to 24 GBd 16-QAM (76 Gb/s net data rate) and 8 GBd 64-QAM (38.4 Gb/s net data rate) deviate less than a factor of two from the maximum distance defined by the reference curves, whereas the transmission of 42 GBd 4-QAM (67.2 Gb/s net data rate) should still be possible at a ~2.6 times larger distance. While we also attribute those implementation penalties of the higher-order modulation formats to device imperfections such as phase noise and nonlinearities, the 42 GBd 4-QAM signal was particularly impaired by the bandwidth limitations of the components due to the broader signal.

The transmission results that use the polarization-division multiplexed system setup are also depicted in Fig. 5. By introducing a second set of Tx/Rx front-ends and antennas, we were able to double the total capacity of the THz-wireless link. Moreover, assuming that each transmitter antenna is aligned to a particular orthogonal polarization mode and that the isolation between them is large enough at the receiver, there is virtually no penalty or interference due to crosstalk.

It needs to be remembered that the introduction of an additional pair of elements does not merely follow the goal of increasing the total capacity of the system, but to enable the simultaneous transmission of the two polarizations of the optical fiber through the air to implement a fully transparent hybrid THz-wireless fiber optic link. Therefore, we also depict in Fig. 5 the result of the short-range, real-time demonstration using a 34 GBd PDM 4-QAM signal with 100 Gb/s net data rate over 0.5 m THz-wireless distance discussed previously. Similarly, we also depicted the successful demonstration of 102.4 Gb/s 4-QAM transmission over 500 m with a BER below the SD-FEC threshold, which represents an important milestone on the way to a realistic implementation of a THz-wireless fiber extender.

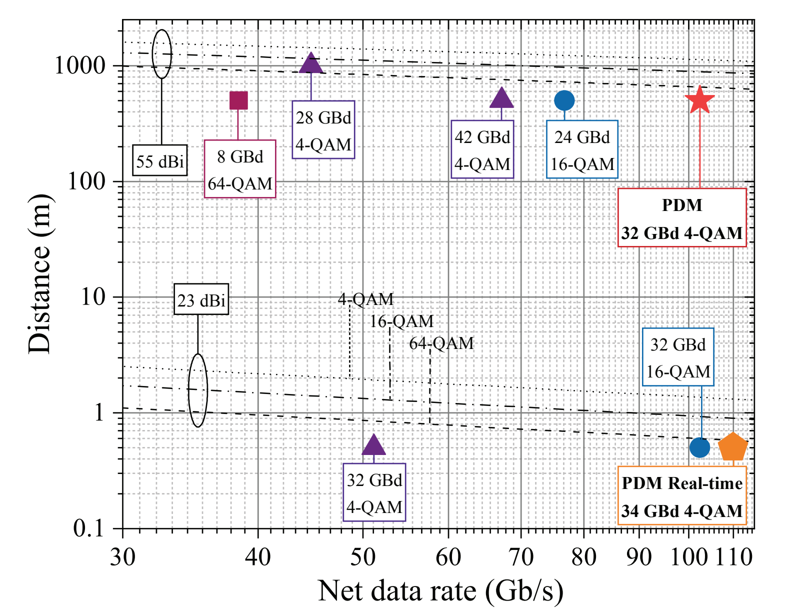

Figure 5. Summary of our high-capacity THz-wireless transmission experiments. The dotted and dashed reference curves for the various *m*-QAM formats depict analytical AWGN calculations of the maximum distance that can be achieved assuming error-free decoding with 25 percent overhead (BER threshold at $3.4 \cdot 10^{-2}$). For the calculations, we have defined a transmit power of −7 dBm, a noise figure of 8 dB at the THz receiver front-end, and an atmospheric loss value of 5 dB/km (clear sunny day). Unless stated otherwise, the experiments in the graph refer to single-pol configuration with offline DSP.

Outlook: THz-Wireless PDM Front-Ends Using Dual-Polarized Antennas

In order to achieve polarization-multiplexed long-range transmission, we introduced a second outdoor unit both at the transmitter and at the receiver. This resulted in a more complex setup, which would be too bulky for bidirectional transmission.

The need for small-sized radio heads, along with the goal of seamlessly connecting to the optical coherent transceivers, has motivated the development of a concept for a 2 × 2 polarization-MIMO frontend. In principle, the two polarizations of the optical fiber, X and Y, can be mapped either to two frequencies, or to two arbitrary, but orthogonal polarizations (H and V) for the THz-wireless transmission. The remaining degree of freedom, either two polarizations or two frequencies, would be used for the separation of the downlink and uplink. For our future work, we prefer to map the two polarizations of the fiber to the vertical (V) and horizontal (H) polarization of the THz-wireless link, as depicted in Fig. 6. After direct IQ-modulation onto the THz carrier, both polarization tributaries are multiplexed to one common circular waveguide that supports two orthogonal modes merging into the Cassegrain antenna feed horn. The advantages of

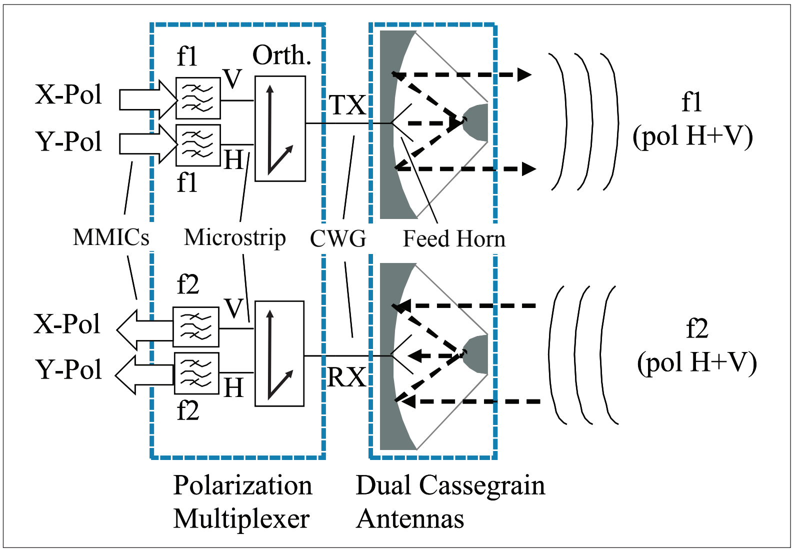

Figure 6. Concept of the THz-wireless PDM front-end for bidirectional transmission. The feed horns of the Cassegrain antennas provide a circular waveguide interface that supports two modes. The band pass filters can be omitted when high-gain antennas are used.

this solution are that there is no need for a frequency diplexer, and the polarization multiplexer requirements are less stringent due to the polarization-MIMO compensation by the DSP. In addition, the scenarios when using high gain antennas enable full duplex operation at the same carrier frequency, which allows the exploitation of twice the bandwidth. The isolation of the Tx and Rx was measured to be better than 90 dB for the two 55 dBi antennas, which provides sufficient isolation for broadband systems.

The developed THz-wireless transceiver modules for the experiments can integrate one of the configurations in a single package: two Tx, two Rx, or an Rx and Tx. Gradually, the modules can be modified and enhanced (i.e., going from the single Tx/Rx case to the polarization-MIMO case) using the same chipset and module integration platform. The front-ends are based on single-chip terahertz monolithic integrated circuits (TMICs) based on 35-nm InGaAs high-electron-mobility transistor (HEMT) technology for the Rx and Tx and the generation of the LO by frequency multiplication. The IQ direct conversion architecture was used for the implementation of the up-converter and down-converter function using a double balance passive mixer.

The reference signal for the 300 GHz carrier is an 8.244 GHz signal, which is generated by a dielectric resonator oscillator (DRO). We estimated the phase noise at a frequency of 1 MHz and measured it to be better than –110 dB/Hz for the LO at 300 GHz. This was derived from measurements at 8.244 GHz and 100 GHz (after frequency multiplication by 12). Furthermore, the thermal phase noise is better than –125 dBc/Hz at a carrier of 300 GHz for frequency offset values larger than 10 MHz. No direct measurement of the phase noise was possible at 300 GHz due to missing equipment. It is important to highlight that the Tx and the Rx sites of the point-to-point link have their own individual reference oscillators, for all the presented lab experiments as well as for all the outdoor long-range transmission experiments. In the lab experiments, two synthesizers were used instead of the DRO solutions. For the outdoor experiments, this means that the fiber optic single-carrier DSP had to correct not only the phase noise but also a larger thermal drift of the LO frequency. Active temperature stabilization of the outdoor units was not considered to simplify the implementation.

Looking at the THz wireless technology challenges that we face, the most important one to be addressed is the linearity of the receiver. It is important to support higher-order modulation schemes (i.e., > 16-QAM) in order to be on par with the evolution of the fiber optic digital-coherent systems. Very low receiver noise figures better than 9 dB can be realized at 300 GHz using high gain low noise amplifiers (LNAs) [15]. However, since the maximum possible LNA gain is limited by the compression of the mixer, these noise figure values have to be traded off with linearity in order to maximize the dynamic range of the receivers. Another important aspect is the functional integration, since there is a need to add more and more control and calibration functions to the THz transceivers, similar to what fiber optic transceivers offer. For this reason, a unified control interface for both the fiber optic and THz-wireless transceivers would be very beneficial for improving the overall combined analog system performance.

Conclusions

We have explored the concept of THz-wireless communications in the 300 GHz band and their integration with high-speed fiber optic transmission systems by means of a transparent, analog optical/RF baseband interface. The implementation of a short-range real-time THz-wireless fiber extender with 100 Gb/s net capacity demonstrated that typical DSP schemes used in fiber optic modems can be applied to jointly compensate for the channel impairments of the combined fiber optic/THz-wireless link. On the way to an integrated solution, it is necessary to show the feasibility of THz-wireless transmission over hundreds of meters first. By implementing a 500-m-long THz-wireless link in Berlin and a 1-km-long THz-wireless link in Freiburg, we were able to investigate the performance of long-range data transmission in the THz band. In addition, we analyzed the impact of changing weather conditions on the transmission performance of a 32 GBd 4-QAM THz-wireless system with a 51.2 Gb/s net capacity. For the 500 m transmission experiment, we achieved a maximum net data rate of 102.4 Gb/s using a PDM configuration (32 GBd PDM 4-QAM). For the 1-km-long link, we confirmed a net data rate of 44.8 Gb/s in a single polarization configuration (28 GBd 4-QAM).

Acknowledgments

This work was supported by the Fraunhofer Internal Programs under Grant No. MAVO 836 966 and by the EC Horizon 2020 Research and Innovation Program under grant agreement No. 761794 (TERRANOVA).

References

[1] "Cisco Annual Internet Report (2018–2023)," White Paper; https://www.cisco.com/c/en/us/solutions/collateral/executive-perspectives/annual-internet-report/white-paper-c11-741490.html, accessed Apr. 29, 2020.

[2] F. Boccardi *et al.*, "Five Disruptive Technology Directions for 5G," *IEEE Commun. Mag.*, vol. 53, no. 2, Feb. 2014, pp. 74–80.
[3] I. F. Akyildiz, J. M. Jornet, and C. Han, "Terahertz Band: Next Frontier for Wireless Communications," *Elsevier Physical Commun.*, vol. 12, pp. 16–32, Feb. 2014.
[4] A.-A. A. Boulogeorgeos *et al.*, "Terahertz Technologies to Deliver Optical Network Quality of Experience in Wireless Systems Beyond 5G," *IEEE Commun. Mag.*, vol. 56, no. 6, June 2018, pp. 144–51.
[5] X. Li *et al.*, "A 400G Optical Wireless Integration Delivery System," *Optics Express*, vol. 21, no. 16, 2013, pp. 187,894–99.
[6] A. Hirata, *et al.*, "120 GHz-Band Wireless Link Technologies for Outdoor 10-Gbit/s Data Transmission," *IEEE Trans. Microw. Theory Techn.*, vol. 60, no. 3, 2012, pp. 881–95.
[7] S. Koenig, *et al.*, "Wireless Sub-THz Communication System With High Data Rate," *Nature Photonics 7*, 2013, pp. 977–81.
[8] T. Nagatsuma, G. Ducournau, and C. C. Renaud, "Advanced in Terahertz Communications Accelerated by Photonics," *Nature Photonics 10*, 2016, pp. 371–79.
[9] C. Castro, R. Elschner, and C. Schubert, "Analysis of Joint Impairment Mitigation in a Hybrid Optic-THz Transmission System," *Proc. 20th IEEE Int'l. Wksp. Signal Processing Advances in Wireless Commun.*, Cannes, France, 2019.
[10] C. Castro *et al.*, "100 Gb/s Real-Time Transmission over a THz Wireless Fiber Extender Using a Digital-Coherent Optical Modem," *Proc. OFC*, San Diego, CA, 2020.
[11] R. Elschner *et al.*, "Experimental Demonstration of a Format-Flexible Single-Carrier Coherent Receiver Using Data-Aided Digital Signal Processing," *Optics Express*, vol. 20, no. 27, Dec. 2012, pp. 28,786–91.
[12] C. Castro *et al.*, "100 Gb/s Terahertz-Wireless Real-Time Transmission Using a Broadband Digital-Coherent Modem," *Proc. IEEE 5G World Forum*, Dresden, Germany, 2019.
[13] C. Castro *et al.*, "Long-Range High-Speed THz-Wireless Transmission in the 300 GHz Band," *Proc. 3rd Int'l. Wksp. Mobile Terahertz Systems*, Essen, Germany, 2020.
[14] ITU-R Rec. P.676-12, "Attenuation by Atmospheric Gases and Related Effects"; https://www.itu.int/rec/R-REC-P.676-12-201908-I/en, Aug. 2019, accessed Apr. 7, 2020.
[15] A. Tessmann *et al.*, "A 300 GHz Low-Noise Amplifier S-MMIC for Use in Next Generation Imaging and Communication Applications," *Proc. 2017 IEEE MTT-S Int'l. Microwave Symp.*, Honolulu, HI, 2017.

Biographies

CARLOS CASTRO (carlos.castro@hhi.fraunhofer.de) received his M.Sc. and Dr.-Ing. (Ph.D.) degrees from Kiel University in Germany in 2014 and 2019, respectively. Since 2018, he has been a research associate at Fraunhofer Heinrich Hertz Institute, Berlin, Germany.

ROBERT ELSCHNER (robert.elschner@hhi.fraunhofer.de) received his Dipl.-Ing. and Dr.-Ing. (Ph.D.) degrees in electrical engineering from Technische Universität Berlin, Germany, in 2006 and 2011, respectively. In 2005, he was with Telecom ParisTech. Since 2010, he has been a member of the scientific staff and project manager at Fraunhofer Heinrich Hertz Institute.

THOMAS MERKLE (thomas.merkle@iaf.fraunhofer.de) received his M.Sc. and Ph.D. degree in Germany from the University of Stuttgart and the University of Ilmenau in 1999 and 2006, respectively. From 2005 to 2010, he worked as a postdoctoral fellow at the CSIRO ICT Centre, Sydney, Australia. From 2010 to 2013, he was a senior research engineer at the Sony STC in Germany. Currently, he is with the Fraunhofer IAF.

COLJA SCHUBERT (colja.schubert@hhi.fraunhofer.de) received his Dipl.-Phys. and Dr.rer.nat. degrees in physics from Technische Universität Berlin in 1998 and 2004, respectively. Since 2000, he has been a member of the scientific staff at Heinrich Hertz Institute. He is currently heading the Submarine and Core Systems group in the Photonic Networks and Systems Department.

RONALD FREUND (ronald.freund@hhi.fraunhofer.de) received Dipl.-Ing. and Dr.-Ing. degrees in electrical engineering from the Technical University of Ilmenau in 1993 and 2002, respectively. Since 1995, he has been with Heinrich Hertz Institute, where he is currently leading the Photonic Network and Systems Department with a focus on network design and modeling, high-capacity submarine and core networks, high-speed access networks, as well as satellite and quantum communication networks. In 2017 he was appointed Professor for Photonic Communication Systems at the Technical University of Berlin. He holds an M.B.A. from RWTH Aachen.